

Supporting Information

Enhanced Quantum Efficiency in Vertical Mixed-thickness n -ReS₂/p-Si Heterojunction Photodiodes

Bablu Mukherjee, ^{*,†} Amir Zulkefli, ^{†,‡} Ryoma Hayakawa, [†] Yutaka Wakayama, ^{†,‡} and Shu Nakaharai^{*,†}

[†] International Center for Materials Nanoarchitectonics (WPI-MANA), National Institute for Materials Science (NIMS), 1-1 Namiki, Tsukuba 305-0044, Japan

[‡] Department of Chemistry and Biochemistry, Faculty of Engineering, Kyushu University, 1-1 Namiki, Tsukuba 305-0044, Japan

*Email: MUKHERJEE.Bablu@nims.go.jp (B.M.), NAKAHARAI.Shu@nims.go.jp (S.N.)

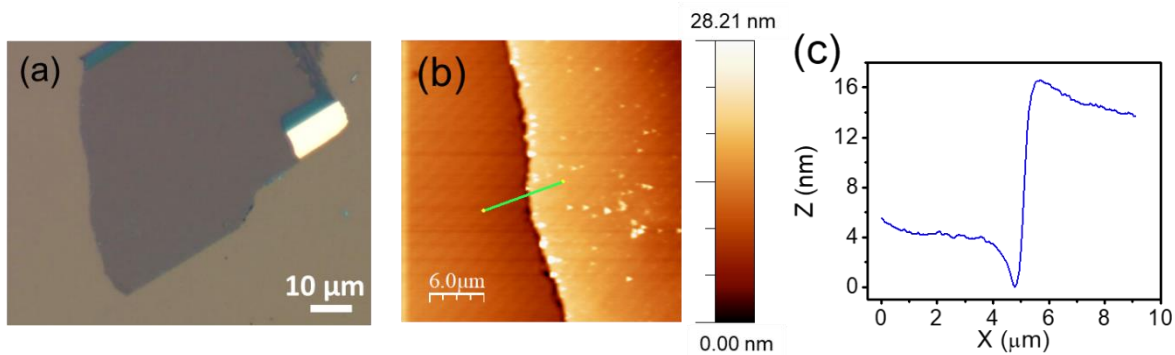


Figure S1. (a) Optical image and (b) surface topography AFM image of the large-area ReS₂ film fabricated using an Au-mediated technique. (c) The line profile of the thickness across the line shown in (b).

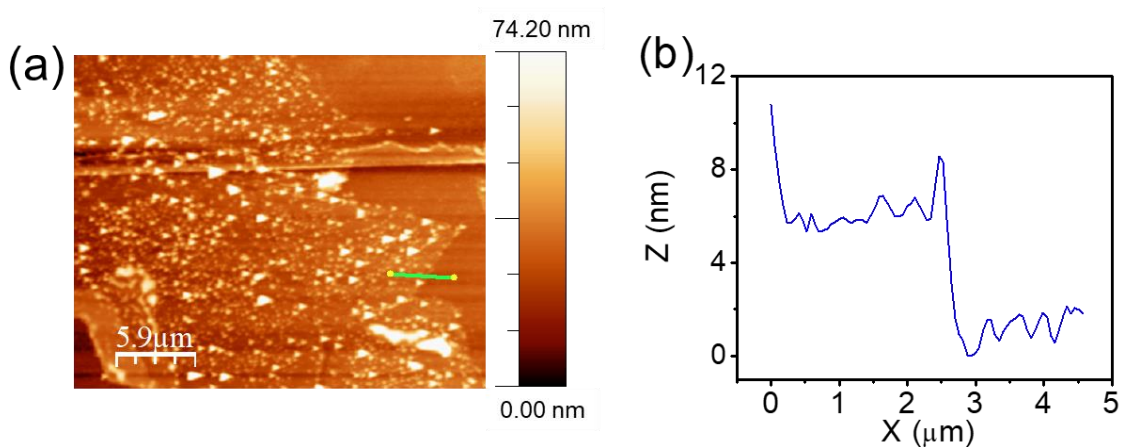


Figure S2. (a) Surface topography AFM image of the uniform few-layer-thick ReS₂ film. (b) The line profile of the thickness across the line shown in (a).

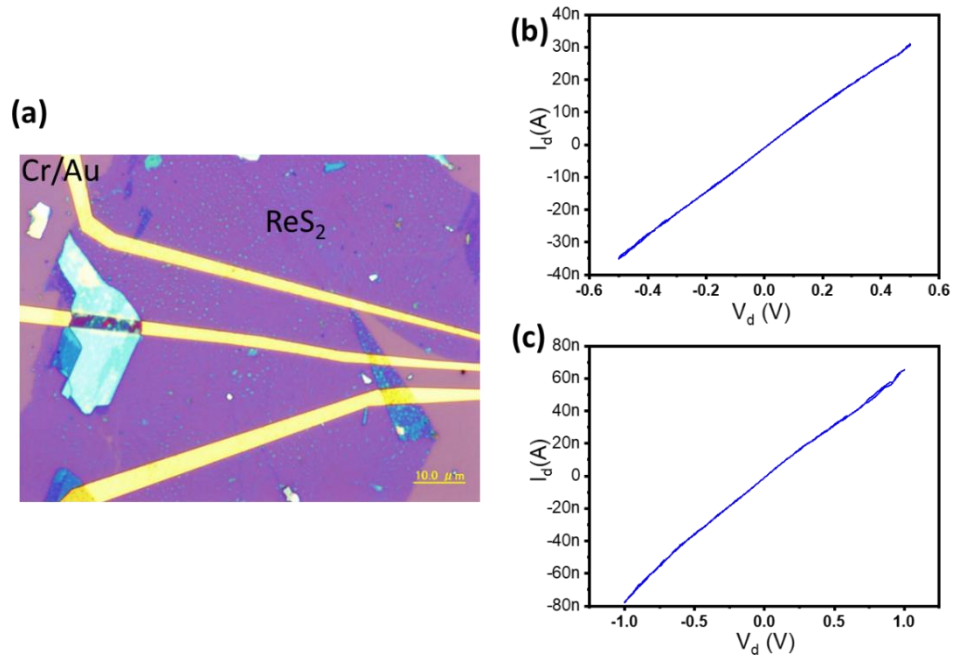


Figure S3. (a) Optical image of a large area, thin ReS₂ film was deposited and sintered at 110 °C under vacuum condition for 30 minutes on top of prefabricated Cr/Au electrodes on SiO₂/Si substrate. (b, c) *I-V* characteristics of the device at two different bias ranges, indicating almost linear *I-V* characteristics of the Au-ReS₂-Au device structure.

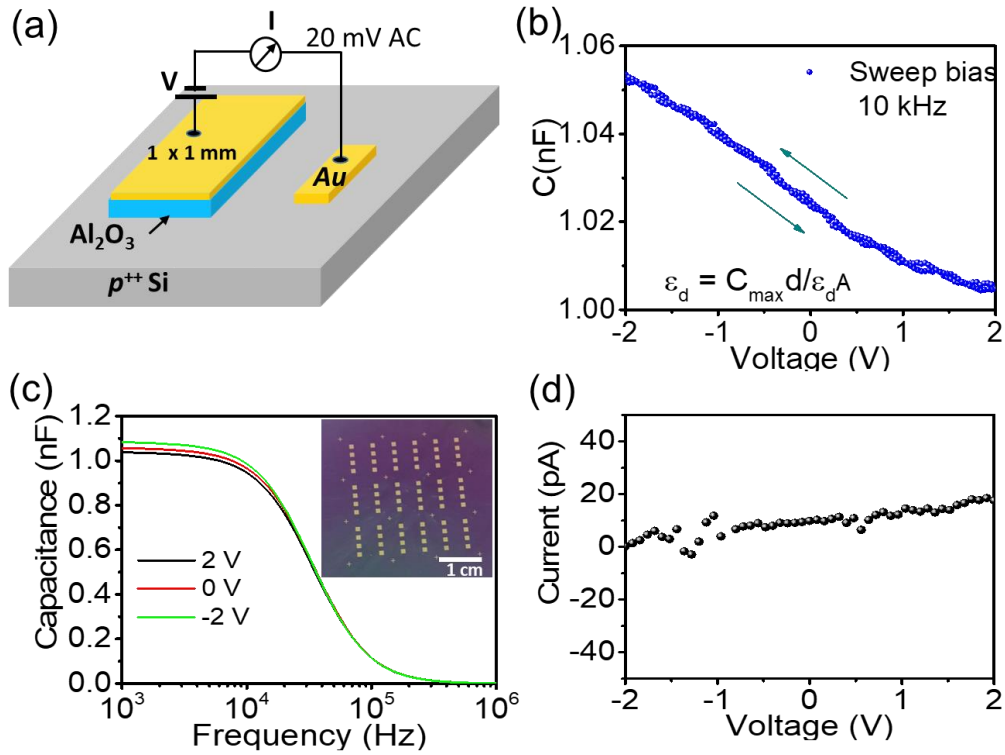


Figure S4. (a) Schematic circuit diagram for measuring the *C-V* and *C-f* characteristics. (b) Sweep *C-V* characteristics indicating no hysteresis width for the absence of fixed oxide charges. (c) *C-f*

characteristics at different biases. The inset shows the image of fabricated patterned $\text{Al}_2\text{O}_3/\text{Cr}/\text{Au}$ squares on top of the $p^{++}\text{Si}$ substrate. (d) I - V curve showing negligible leakage current through the Al_2O_3 oxide layer.

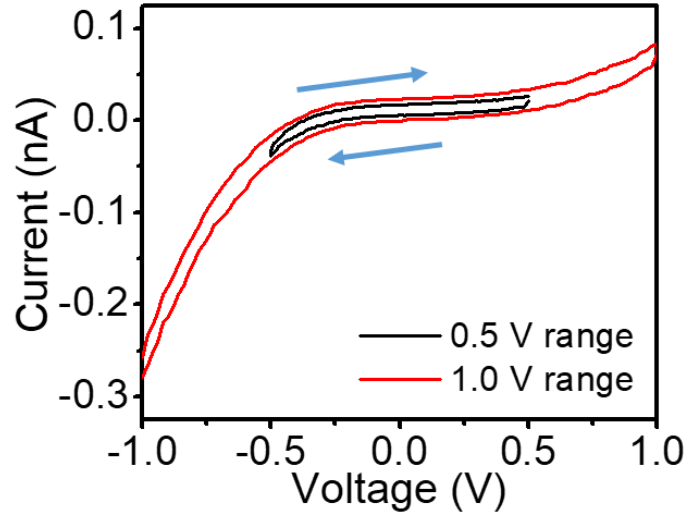


Figure S5. Sweep $I_{\text{DS}}-V_{\text{DS}}$ for different bias ranges showing hysteresis.

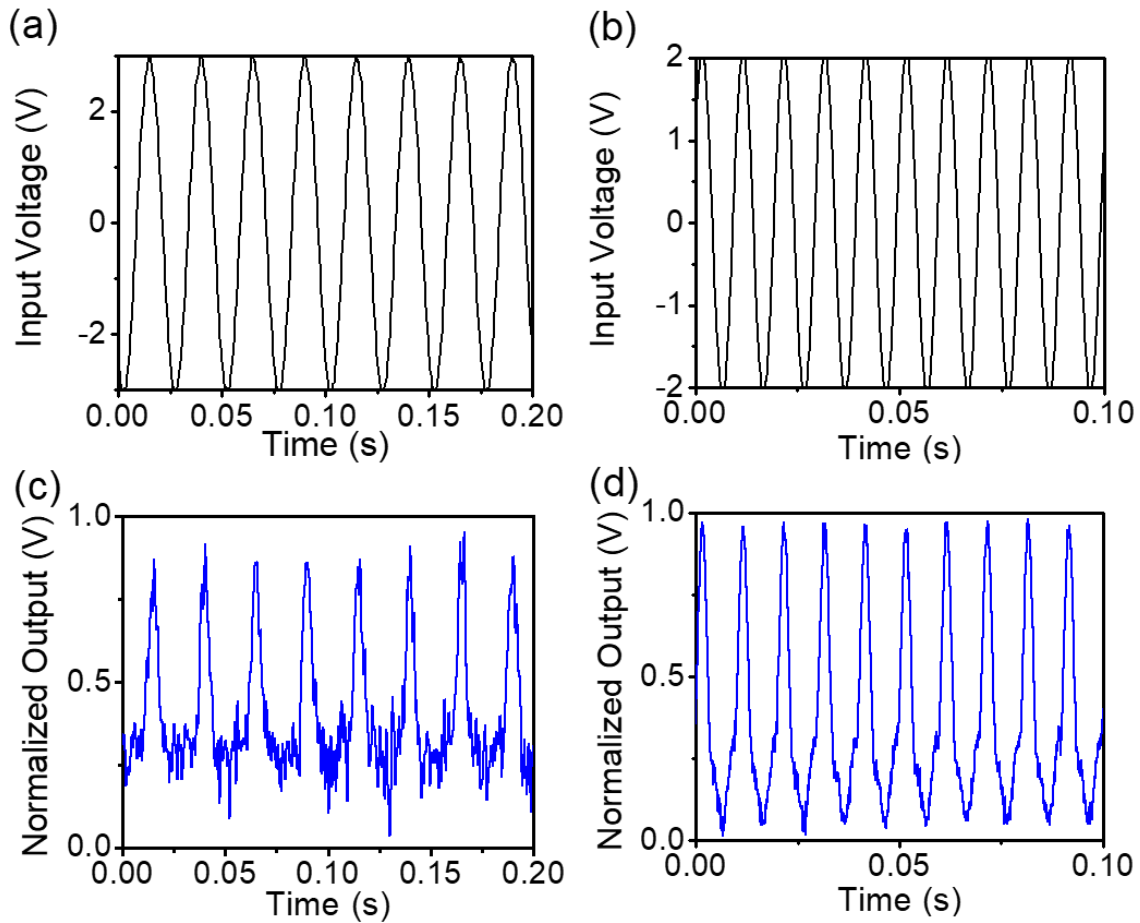


Figure S6. Rectification characteristics of the heterojunction diode for (a, b) 40 Hz and (c, d) 100 Hz.

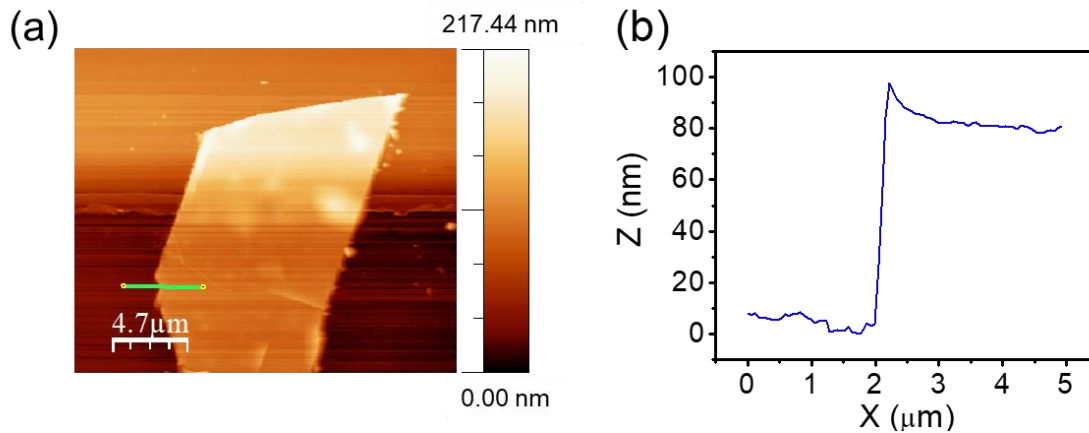


Figure S7. (a) Surface topography AFM image of the uniform multilayer-thick ReS₂ film. (b) The line profile of the thickness across the line shown in (a).

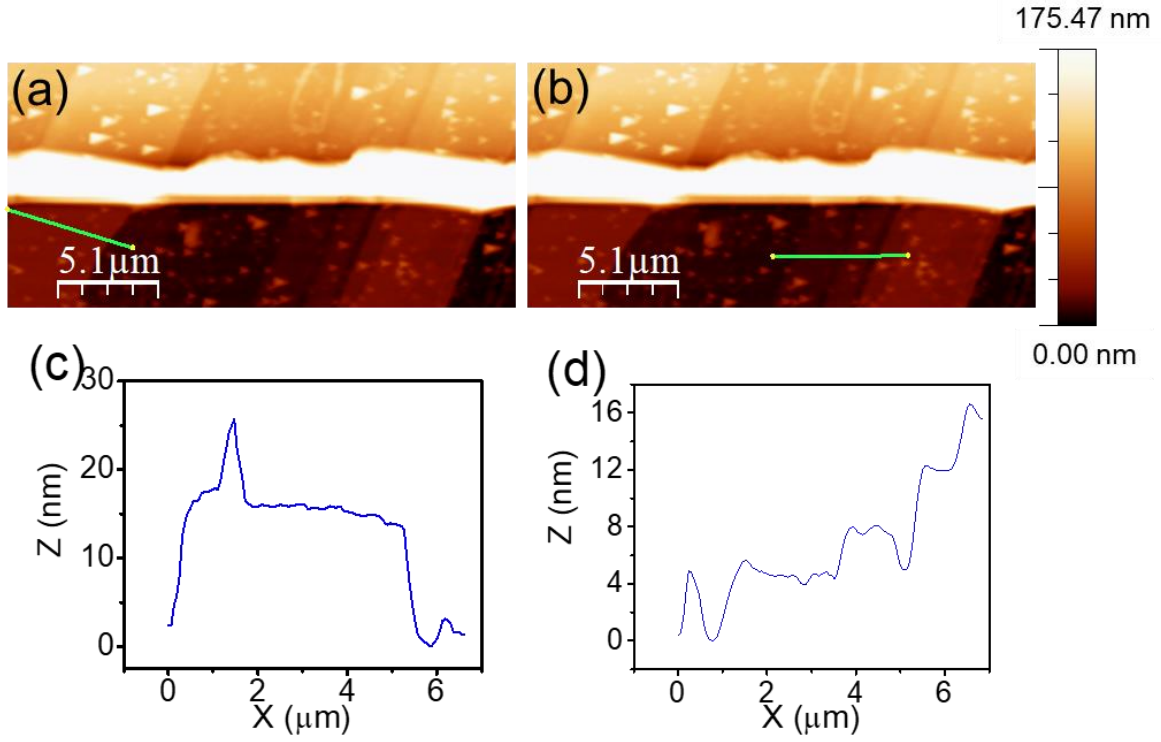


Figure S8. (a) Surface topography AFM image of the nonuniform few-layer-thick mixed-thickness ReS₂ film. (b) The line profile of the thickness across the line shown in (a).

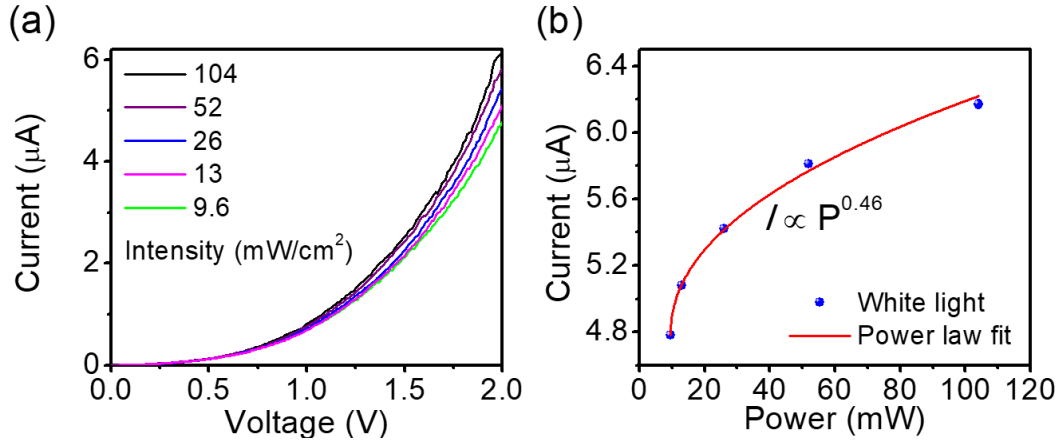


Figure S9. (a) Mixed-thickness ReS₂/Si heterostructure device: I - V characteristics with different powers under white-light illumination and (b) the power-law dependence at 2 V operation.

Device Photodiode	Wavelength and bias	Photoresponsivity (A/W)	Response time	Reference
Graphene/Si	500 nm, 2 V	~0.12	-	[15]
Monolayer MoS ₂ /Si	365 nm, 4 V	~0.7	-	[9]
Multilayer MoS ₂ /Si	800 nm, 0 V	~0.3	~3 μ s	[11]
WS ₂ /Si	631 nm, 2 V	~1.15	42 ms	[17]
Multilayer ReS ₂ /Si	633 nm, 1 V	~0.004	20 μ s	[28]
Mixed-thickness ReS₂/Si	532 nm, 3 V	~33.47	80 μs	Presented work

Table S1: Comparison of the presented work with those reported for 2D-material-based photodiodes.

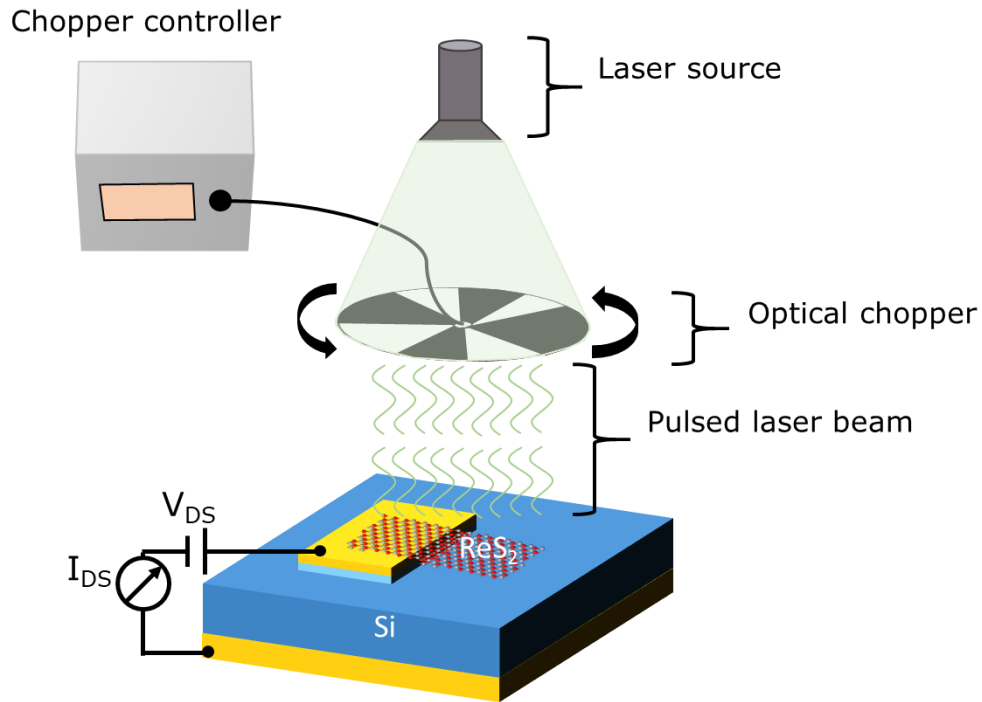


Figure S10. Schematic of the pulsed photocurrent–time measurement setup.

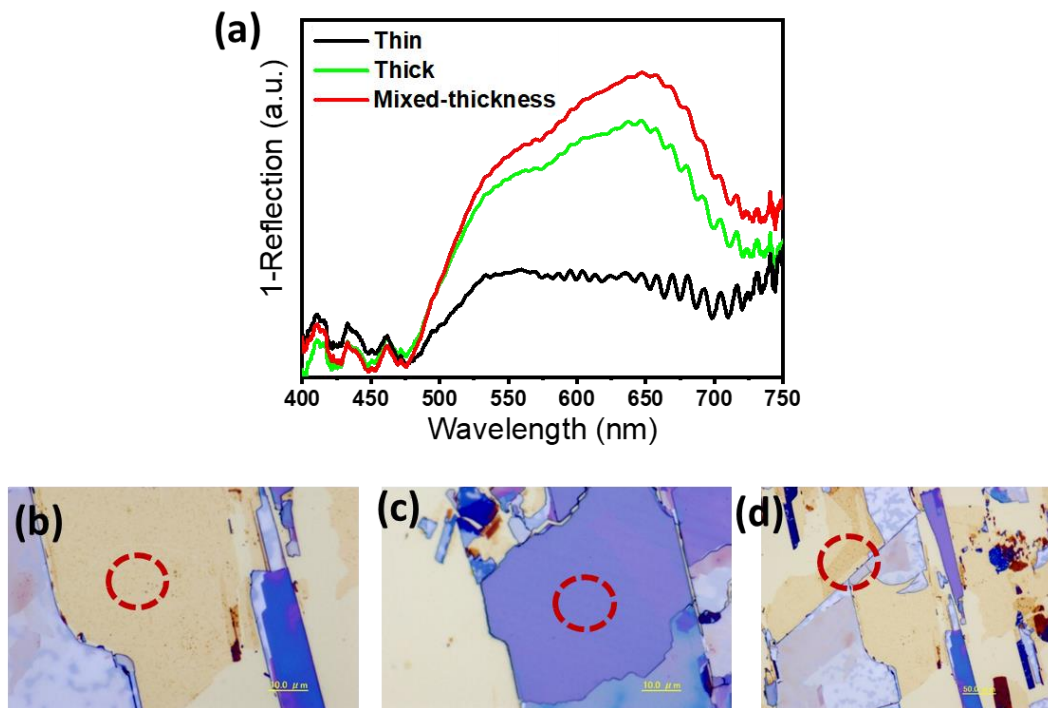


Figure S11. (a) Absorption spectra of the ReS₂ sample as shown in the optical images, (b) thin, (c) thick and (d) mixed-thickness on top of Au film coated substrate.